^{18}F-NOTA-FAPI-04 uptake in metastatic lesions on PET/CT imaging can distinguish different pathological types of lung cancer

Yuchun Wei
Shandong University
Kai Cheng
Shandong Cancer Hospital and Institute
Zheng Fu
Shandong Cancer Hospital and Institute
Jinsong Zheng
Shandong Cancer Hospital and Institute
Zhengshuai Mu
Shandong Cancer Hospital and Institute
Chenglong Zhao
Shandong Cancer Hospital and Institute
Xiaoli Liu
Shandong University
Shijie Wang
Shandong Cancer Hospital and Institute
Jinming Yu
Shandong Cancer Hospital and Institute
Shuanghu Yuan (yuanshuanghu@sina.com)
Shandong Cancer Hospital affiliated to Shandong University https://orcid.org/0000-0002-3857-2800

Research Article

Keywords: Fibroblast activation protein, FAPI, PET/CT, lung cancer

Posted Date: August 13th, 2021

DOI: https://doi.org/10.21203/rs.3.rs-791998/v1

Abstract

Purpose

Radionuclide-labeled fibroblast-activation-protein inhibitor 04 (FAPI-04) as a positron emission tomography (PET) imaging tracer can reveal the localized expression of fibroblast activation protein (FAP), a cell-surface serine protease that is highly upregulated in more than 90% of epithelial carcinomas. In this study, we quantified the ^{18}F-NOTA-FAPI-04 uptake on PET/computed tomography (CT) imaging in different pathological types of lung cancer and metastatic tumors.

Methods

We prospectively enrolled 61 patients with histopathologically proven primary lung cancer with metastases.PET/CT scanning was performed before any antitumor therapy and 1hour after injection of 235.10 ± 3.89 MBq of ^{18}F-NOTA-FAPI-04. Maximum standard uptake values (SUV_{max}) were calculated for comparison among primary and metastatic lesions.

Results

Sixty-one patients with adenocarcinoma (ADC, n = 30), squamous cell carcinoma (SCC, n = 17), and small cell lung cancer (SCLC, n = 14) were enrolled in this study, and 61 primary tumors and 199 metastases were evaluated. No difference in^{18}F-NOTA-FAPI-04 uptake was observed among primary ADC, SCC, and SCLC tumors ($P = 0.198$).Additionally, no difference in uptake was found between primary and metastatic lesions of lung cancer with the same pathological type ($P > 0.05$).However, uptake did differ among metastases of differing pathological type ($P < 0.001$). The SUV_{max} of metastatic lymph nodes was highest for SCC, followed by ADC and then SCLC ($P < 0.001$).The SUV_{max} of bone metastases also was highest for SCC, followed by ADC and SCLC ($P < 0.05$), but no difference was observed between ADC and SCLC. The SUV_{max} of metastases in other organs was higher in SCC cases than in ADC cases, but did not differ between SCC and SCLC or ADC and SCLC. Bone metastases exhibited higher uptake than those of lymph nodes and other organs in SCC and ADC ($P < 0.05$), but not in SCLC.

Conclusion

^{18}F-NOTA-FAPI-04 PET/CT imaging revealed differences in FAP expression in metastases of lung cancer, with the highest expression specifically in bone metastases, and thus, may be valuable for distinguishing different pathological types of lung cancer.

Introduction

Lung cancer is the most commonly diagnoses and deadliest cancer worldwide. About 40% of cases are diagnosed at an advanced stage, and the 5-year survival rate of patients with advanced lung cancer is less than 10% [1, 2]. Given the high mortality rate associated with lung cancer, a comprehensive understanding of the key biological characteristics closely related to the efficacy of lung cancer treatments is of great significance to improving outcomes among lung cancer patients.

Fibroblast activation protein (FAP) is a membrane-anchored peptidase that belongs to the dipeptidyl peptidase 4 (DPP4) families and has dipeptidyl peptidase and endopeptidase activities [3]. FAP expression has been reported on the surface of tumor stromal cells, macrophages, and tumor cells [4]. It is highly expressed in more than 90% of epithelial tumors [5], but expressed at low levels in physiological conditions [6, 7]. For this reason, it is often used as a marker of pro-tumorigenic stroma [8]. In healthy tissues, the stroma mainly acts as a barrier against tumor formation. However, the presence of tumor cells can transform the stroma into an environment that is conducive to tumor growth [9, 10]. The co-evolution and continuous participation of the stroma and tumor cells in the process of tumorigenesis are the main reasons for the heterogeneity of the tumor microenvironment.

Radionuclide-labeled fibroblast-activation-protein inhibitor (FAPI) can specifically bind with FAP, and thus, its use inpositron emission tomography (PET)/computed tomography (CT) imaging can allow thedetection of FAP in the tumor microenvironment, providing insight into the biological characteristics of tumors. In this study, we quantified the tumor uptake on ^{18}F-NOTA-FAPI-04 on PET/CT for different pathological types of lung cancer and metastatic tumors to characterize FAP expression in lung cancer.

Materials And Methods

Patients

Sixty-one lung cancer patients with adenocarcinoma (ADC, 30/61), squamous cell carcinoma (SCC, 17/61), or small cell lung cancer (SCLC, 14/61) were randomly recruited from December 2020 to June 2021 before the administration of any anti-tumor therapy. Our investigation was performed under the conditions of the updated Declaration of Helsinki (unproven interventions in clinical practice). This prospective study was approved by the local ethics committee of Shandong Cancer Hospital and Institute, and each patient provided written and informed consent for inclusion in the study.

^{18}F-NOTA-FAPI-04 PET/CT scanning

Fasting and blood glucose measurement were not required or requested before imaging examinations. Patients received an intravenous injection of 4.81 MBq/kg (0.12 mCi/kg) ^{18}F-NOTA-FAPI-04 and then rested for approximately 60 minutes. Scanning was then performed with an integrated in-line PET/CT system (GEMINI TF Big Bore; Philips Healthcare, Cleveland, OH, USA). PET images were obtained from the head to the thigh, and the spiral CT component was performed with an X-ray tube voltage peak of 120 kV, 300 mAs. A full-ring dedicated PET scan of the same axial range followed. The patients continued normal shallow respiration during image acquisition.

Imaging analysis

The images were attenuation-corrected with the transmission data from CT. The attenuation-corrected PET images, CT images, and fused PET/CT images, which were displayed as coronal, sagittal, and trans axial slices, were viewed and analyzed on a Nuclear Medical Information System (Beijing Mozi Healthcare Ltd., Beijing, China).

Tumor tracer uptake was quantified according to the maximum standard uptake value (SUV_{max}) at 1 hour after injection. For calculation of the SUV, circular regions of interest (ROIs) were drawn around the tumor lesions with a focally increased uptake in transaxial slices and automatically adapted to a 3-dimensional volume with a 30% isocontour.

Immunohistochemistry

Immunohistochemical staining was performed to confirm FAP expression in the tumor tissues. Tissues obtained by biopsy were formalin-fixed and paraffin-embedded before beingcut into 3- to 5-μm-thick sections on a macrotome (Microm HM 450; GMI, Ramsey, MN, USA). The sections were then immunostained with a FAP-alpha antibody (1:100 dilution, ab53066; Abcam, Cambridge, MA, USA).

Statistical analysis

Data for continuous variables are presented as mean±standard error (SE) values. SUVs were compared among histopathological types of lung cancer using one-way analysis of variance (ANOVA). SUVswere compared between primary tumors and metastases using independent sample t tests.A *P* value less than 0.05 was considered statistically significant. All analyses were performed using Prism 9.1.2 (GraphPad, San Diego, CA, USA).

Results

From December 2020 to June 2021, 61 patients diagnosed with lung cancer based on histological examinations at Shandong Cancer Hospital and Institute were enrolled in this study. A total of 61 primary tumors and 199 metastatic lesions were evaluated. The patients' characteristics are presented in Table 1.

^{18}F-NOTA-FAPI-04 uptake in primary tumors of differing pathological type and comparison of uptake between primary and metastatic lesions

The SUV_{max} of ^{18}F-NOTA-FAPI-04 in primary tumors did not differ significantly among SCC (9.31±0.99), ADC (7.36±0.86), and SCLC (6.65±1.02) tumors (*P*>0.05; **Table 2** and **Fig. 1-a**). Additionally, ^{18}F-NOTA-FAPI-04 uptake values in primary and metastatic lesions were comparable in patients with the same pathological type of lung cancer (**Fig. 1-b, c, d and Fig. 2**).

Comparison of ^{18}F-NOTA-FAPI-04uptake between metastasesof the same organs in patients with different pathological types of lung cancer

A significant difference in the SUV_{max} of ^{18}F-NOTA-FAPI-04 was observed among metastases of different pathological types of lung cancer (P<0.001; **Fig. 3-a**). Metastases from SCC showed the highest SUV_{max} (10.41±1.39), followed by ADC (7.03±0.37) and then SCLC (4.94±2.60). The differences between each pair of pathological types were all significant, with P values of 0.0019, <0.0001, and 0.033 for the comparisons of SCC vs. ADC, SCC vs. SCLC, and ADC vs. SCLC, respectively.

For bone metastases (**Fig. 3-b**), the SUV_{max} of metastases from SCC (20.50 ±9.19) was significantly higher than the SUV_{max} of metastases from ADC (9.14 ±0.76; P=0.0036) or SCLC (5.52 ±1.10; 0.0004). No significant difference was observed between the uptake values in bone metastases from ADC and SCLC (P=0.1273).

For lymph node metastases (**Fig. 3-c**), the SUV_{max} of metastatic lymph nodes from SCC (9.04 ±0.67) was higher than that of metastatic lymph nodes from ADC (6.61 ±0.45; P=0.0208) or SCLC (4.41 ±0.43; P=0.0001). Additionally, the SUV_{max} of metastatic lymph nodes was higher for ADC than SCLC (P=0.0256).

For metastases in other organs, including brain, lung, adrenal gland, liver, pleura, peritoneum, and soft tissue (**Fig. 3-d**), the SUV_{max} in metastatic lesions from SCC was 9.02±2.60, which was higher than that in metastases from ADC (4.84±0.56; P=0.0299) but not significantly different from that in metastases from SCLC (5.50±0.55; P>0.05).The SUV_{max} in metastatic lesions from ADC and SCLC also did not differ significantly.

Comparison of ^{18}F-NOTA-FAPI-04 uptake between metastases of different organs in patients with the same pathological type of lung cancer

In patients with SCC, the SUV_{max} for bone metastases, lymph node metastases and metastases in other organs were 20.05±9.19, 9.04±0.67, and 9.02±2.60, respectively (**Fig. 4-a** and **Fig. 5**). The SUV_{max} in bone metastases was higher than the uptake values in lymph node metastases (P=0.018) or metastases in other organs (P=0.036), while the uptake values did not differ significantlybetween lymph node metastases or metastases in other organs (P>0.99).

Consistent results were obtained in patients with ADC (**Fig. 4-b**). The highest SUV_{max} was observed for bone metastases (9.14±0.76), and this value was significantly higher than those in lymph node metastases (6.61±0.45; P=0.0049) and metastases in other organs (4.84±0.56; P<0.0001). Again, no significant difference in ^{18}F-NOTA-FAPI-04 uptake was observed between metastases in lymph nodes and other organs (P=0.119).

Different from the results obtained in ADC and SCC cases, the ^{18}F-NOTA-FAPI-04 uptake values in bone metastases, metastatic lymph nodes, and metastases in other organs in patients with SCLC were 5.52±1.10, 4.41±0.43 and 5.50±0.55, respectively, with no significant differences between them (all P>0.05; **Fig. 4-c**).

Discussion

In this study, differences in ^{18}F-NOTA-FAPI-04 uptake were observed among metastatic lung cancer lesions in different sites, which provides insights into the characteristics of FAP expression in the tumor microenvironment of lung cancer and can be helpful for distinguishing different pathological types of lung cancer via PET/CT imaging.

The results of this study showed no differences in ^{18}F-NOTA-FAPI-04 uptake in primary lung tumors of different pathological types. To better characterize the natural expression of FAP in lung cancer, the lung cancer patients enrolled in this study had not yet received any anti-tumor therapy at the time of PET/CT imaging. The uptake values in primary tumors were lower than those reported previously for lung cancer (average SUV_{max}>11) [11, 12]*)*, but the previous studies included some patients who had already received treatment. Thus, it remained unclear whether the uptake values reported in previous studies included metastatic tumors. No related studies on FAPI-04 uptake in patients with different pathological types of lung cancer were found in the literature prior to the present study.

Using FAP-specific PET imaging may allow non-invasive distinction of lung cancer pathological types between SCC, ADC, and SCLC. In this study, we found that the ^{18}F-NOTA-FAPI-04 uptake values in metastases from SCC were the highest, followed by uptake values in metastases from ADC, with the lowest uptake values observed in metastases from SCLC. Lung cancer metastasis is a complex process that begins with the implantation of tumor cells and their interaction with stroma [9]. Then quiescent fibroblasts differentially respond to damage and become activated to support repair. These differentiated fibroblasts are called cancer-associated fibroblasts (CAFs) and can significantly promote tumorigenesis [13]. The process of tumor metastasis occurs in the context of considerable tumor heterogeneity. A previous study found that increased tracer uptake on FAP-specific imaging had the ability to distinguish isocitrate dehydrogenase (IDH)-wild type glioblastomas and high-grade IDH-mutant astrocytoma [14]. In addition, ^{68}Ga-FAPI-04 uptake showed a high sensitivity for distinguishing poorly differentiated hepatic malignancies, with the results confirmed by pathology [15]. Therefore, FAP-specific imaging in tumors may be useful for follow-up studies.

Patients with advanced lung cancer have local and distant tissue and organ metastases. FAP is often highly expressed in the pathophysiological process of the desmoplastic response. SCLC exhibits poor differentiation, a high degree of malignancy and rapid development [16, 17]. Although it is typically diagnosed in an advanced stage, the expression levels of FAP in different metastatic lesions usually have not reached a significant level ofvariance, which may be the reason no significant difference in FAPI-04 uptake was observed among metastases from SCLC. The growth patterns of SCC and ADC originate in epithelial cells and mostly involve accumulative growth, often showing solid density [18-20]. Well-differentiated SCC is associated with a good prognosis [21, 22], and metastasis typically occurs over a long time, resulting in differential expression of FAP in metastases of different organs and tissues.

Bone metastasis is common in patients with advanced lung cancer, with the reported incidence of bone metastasis in non-small cell lung cancer ranging from 30%–55% [23, 24]. In extensive small cell lung cancer, about 40% of patients have bone metastasis [25]. In the present study, patients with ADC and SCLC often had multiple systemic metastases, and FAPI-04 uptake in bone metastases was higher than that in other tissues and organs. At present, radiotherapy combined with opioid analgesia is commonly used in the clinical treatment of bone metastasis, but it can only partially or temporarily relieve the symptoms of metastatic lesions. FAPI-04 was reported to be a promising tracer for both imaging and improving the potency of targeted treatment in cancer patients [26]. ^{68}Ga-FAPI-04 PETCT scans present high absorbance in lesions associated with metastases of breast cancer, and pain symptoms were found to decrease with the use of a low dose of ^{90}Y-FAPI-04 [27]. Theranostic targeting of FAP in the tumor stroma provides a new therapeutic idea for the treatment of patients with systemic metastases including multiple bone metastases and metastases in other tissues and organs.

Due to the limitations of this study, such as the small number of patients and the resultant inability to compare the SUVs of some of metastases tumors for individual cancers, further studies are required to confirm the ability to distinguish pathological lung cancer types based on^{18}F-NOTA-FAPI-04 uptake values in metastases on PET/CT imaging.

Conclusion

18F-NOTA-FAPI-04 PET/CT imaging revealed differential expression of FAP in metastases of lung cancer, especially in bone metastases, with no differences in uptake values observed among primary tumors of different pathological types of lung cancer. Thus, PET/CT imaging with this tracer may be valuable in planning therapeutic regimens for patients with advance lung cancer.

Declarations

Funding: The study was supported by funds from the Major Scientific and Technological Innovation Projects of Shandong (2018YFJH0502), the Academic Promotion Program of Shandong First Medical University (2019ZL002) and the foundation of National Natural Science Foundation of China (81872475, 81372413, 81627901 and 82030082).

Conflicts of interest: No potential conflicts of interest were disclosed.

Availability of data and material: The datasets used or analysed during the current study are available from the corresponding author on reasonable request.

Code availability: All software applications or custom code are available in the public repository.

Authors' contributions: Shuanghu Yuan and Jinming Yu conceived of the study and participated in its designed. Yuchun Wei participated in the experiments and drafted the manuscript. Kai Cheng is responsible for the preparation of [^{18}F]-NOTA-FAPI-04 and [^{18}F]-FDG. Xiaoli Liu and Shijie Wang are

responsible for collecting PET/CT images. Zheng Fu and Jinsong Zheng carried out the nuclear medicine. Zhengshuai Mu and Chenglong Zhao carried out the pathology. All authors read and approved the final manuscript.

Ethics approval and consent to participate: This study was approved by the local ethics committee of Shandong Cancer Hospital and Institute, and the patient gave written and informed consent before the study.

Consent for publication: All authors of the current manuscript meet the specified criteria for authorship and agreed to publish.

Acknowledgments: The authors thank Laney Webber for English language editing services.

References

1. Bray F, Ferlay J, Soerjomataram I, Siegel RL, Torre LA, Jemal A. Global cancer statistics 2018: GLOBOCAN estimates of incidence and mortality worldwide for 36 cancers in 185 countries. CA Cancer J Clin. 2018;68:394–424.
2. Siegel RL, Miller KD, Jemal A. Cancer statistics, 2020. CA Cancer J Clin. 2020;70:7–30.
3. Hamson EJ, Keane FM, Tholen S, Schilling O, Gorrell MD. Understanding fibroblast activation protein (FAP): substrates, activities, expression and targeting for cancer therapy. Proteomics Clin Appl. 2014;8:454 – 63.
4. Loktev A, Lindner T, Mier W, Debus J, Altmann A, Jäger D, et al. A Tumor-Imaging Method Targeting Cancer-Associated Fibroblasts. J Nucl Med. 2018;59:1423-9.
5. Scanlan MJ, Raj BK, Calvo B, Garin-Chesa P, Sanz-Moncasi MP, Healey JH, et al. Molecular cloning of fibroblast activation protein alpha, a member of the serine protease family selectively expressed in stromal fibroblasts of epithelial cancers. Proc Natl Acad Sci U S A. 1994;91:5657-61.
6. Garin-Chesa P, Old LJ, Rettig WJ. Cell surface glycoprotein of reactive stromal fibroblasts as a potential antibody target in human epithelial cancers. Proc Natl Acad Sci U S A. 1990;87:7235-9.
7. Roberts EW, Deonarine A, Jones JO, Denton AE, Feig C, Lyons SK, et al. Depletion of stromal cells expressing fibroblast activation protein-α from skeletal muscle and bone marrow results in cachexia and anemia. J Exp Med. 2013;210:1137-51.
8. Jacob M, Chang L, Puré E. Fibroblast activation protein in remodeling tissues. Curr Mol Med. 2012;12:1220-43.
9. Hanahan D, Coussens LM. Accessories to the crime: functions of cells recruited to the tumor microenvironment. Cancer Cell. 2012;21:309 – 22.
10. Egeblad M, Nakasone ES, Werb Z. Tumors as organs: complex tissues that interface with the entire organism. Dev Cell. 2010;18:884–901.

11. Kratochwil C, Flechsig P, Lindner T, Abderrahim L, Altmann A, Mier W, et al. 68Ga-FAPI PET/CT: Tracer Uptake in 28 Different Kinds of Cancer. J Nucl Med. 2019;60:801-5.
12. Chen H, Pang Y, Wu J, Zhao L, Hao B, Wu J, et al. Comparison of [68Ga]Ga-DOTA-FAPI-04 and [18F] FDG PET/CT for the diagnosis of primary and metastatic lesions in patients with various types of cancer. Eur J Nucl Med Mol Imaging. 2020;47:1820-32.
13. Orimo A, Gupta PB, Sgroi DC, Arenzana-Seisdedos F, Delaunay T, Naeem R, et al. Stromal fibroblasts present in invasive human breast carcinomas promote tumor growth and angiogenesis through elevated SDF-1/CXCL12 secretion. Cell. 2005;121:335 – 48.
14. Röhrich M, Loktev A, Wefers AK, Altmann A, Paech D, Adeberg S, et al. IDH-wildtype glioblastomas and grade III/IV IDH-mutant gliomas show elevated tracer uptake in fibroblast activation protein-specific PET/CT. Eur J Nucl Med Mol Imaging. 2019;46:2569-80.
15. Shi X, Xing H, Yang X, Li F, Yao S, Zhang H, et al. Fibroblast imaging of hepatic carcinoma with 68Ga-FAPI-04 PET/CT: a pilot study in patients with suspected hepatic nodules. Eur J Nucl Med Mol Imaging. 2021;48:196–203.
16. Travis WD, Brambilla E, Noguchi M, Nicholson AG, Geisinger KR, Yatabe Y, et al. International association for the study of lung cancer/american thoracic society/european respiratory society international multidisciplinary classification of lung adenocarcinoma. J Thorac Oncol. 2011;6:244 – 85.
17. Yoshizawa A, Motoi N, Riely GJ, Sima CS, Gerald WL, Kris MG, et al. Impact of proposed IASLC/ATS/ERS classification of lung adenocarcinoma: prognostic subgroups and implications for further revision of staging based on analysis of 514 stage I cases. Mod Pathol. 2011;24:653 – 64.
18. Hirano T, Franzén B, Kato H, Ebihara Y, Auer G. Genesis of squamous cell lung carcinoma. Sequential changes of proliferation, DNA ploidy, and p53 expression. Am J Pathol. 1994;144:296–302.
19. Satoh Y, Ishikawa Y, Nakagawa K, Hirano T, Tsuchiya E. A follow-up study of progression from dysplasia to squamous cell carcinoma with immunohistochemical examination of p53 protein overexpression in the bronchi of ex-chromate workers. Br J Cancer. 1997;75:678 – 83.
20. Sousa V, Bastos B, Silva M, Alarcão AM, Carvalho L. Bronchial-pulmonary adenocarcinoma subtyping relates with different molecular pathways. Rev Port Pneumol (2006). 2015;21:259 – 70.
21. Fang B, Mehran RJ, Heymach JV, Swisher SG. Predictive biomarkers in precision medicine and drug development against lung cancer. Chin J Cancer. 2015;34:295–309.
22. Song Z, Zhu H, Guo Z, Wu W, Sun W, Zhang Y. Correlation of EGFR mutation and predominant histologic subtype according to the new lung adenocarcinoma classification in Chinese patients. Med Oncol. 2013;30:645.
23. Santini D, Daniele S, Barni S, Sandro B, Intagliata S, Salvatore I, et al. Natural History of Non-Small-Cell Lung Cancer with Bone Metastases. Sci Rep. 2015;5:18670.
24. Tsuya A, Kurata T, Tamura K, Fukuoka M. Skeletal metastases in non-small cell lung cancer: a retrospective study. Lung Cancer. 2007;57:229 – 32.

25. Mitsuhashi A, Okuma Y, Zenke Y, Hosomi Y. Prognostic effects of osteoclast inhibitors in extensive stage small cell lung cancer patients with bone metastases. Mol Clin Oncol. 2018;9:561-5.
26. Watabe T, Liu Y, Kaneda-Nakashima K, Shirakami Y, Lindner T, Ooe K, et al. Theranostics Targeting Fibroblast Activation Protein in the Tumor Stroma: 64Cu- and 225Ac-Labeled FAPI-04 in Pancreatic Cancer Xenograft Mouse Models. J Nucl Med. 2020;61:563-9.
27. Lindner T, Loktev A, Altmann A, Giesel F, Kratochwil C, Debus J, et al. Development of Quinoline-Based Theranostic Ligands for the Targeting of Fibroblast Activation Protein. J Nucl Med. 2018;59:1415-22.

Tables

Table 1 Characteristics of the lung cancer patients (*n*=61)

Age, mean ± SE (range)	61.52±9.05 (37–83)
Male, n (%)	45 (73.77%)
Female, n (%)	16 (26.23%)
Pathological type, n (%)	
ADC	30 (49.18%)
SCC	17 (27.87%)
SCLC	14 (22.95%)
Primary tumors, n	61
Metastases, n	199

SE, standard error; SCC, squamous cell carcinoma; ADC, adenocarcinoma; SCLC, small cell lung carcinoma.

Table 2 SUV_{max} of primary tumors and metastases of different pathological types

	ADC	SCC	SCLC	*P*
Primary tumors	7.36±0.86 (n=30)	9.31±0.99 (n=17)	6.65±1.02 (n=14)	0.198
Metastases	7.03±0.37 (n=137)	10.41±1.39 (n=25)	4.94±2.60 (n=37)	<0.001
Lymph node	6.61±0.45 (n=63)	9.04±0.67 (n=16)	4.41±0.43 (n=19)	<0.001
Bone	9.14±0.76 (n=44)	20.50±9.19 (n=3)	5.52±1.10 (n=12)	<0.001
Liver	3.76±0.65 (n=3)	3.38±0.49 (n=2)	5.12±1.07 (n=3)	0.039
Brain	3.03±0.60 (n=7)	17.66 (n=1)	5.16 (n=1)	
Adrenal gland	6.24±1.82 (n=6)	11.78 (n=1)	/	
Pleura	5.44±1.27 (n=7)	8.95±5.28 (n=2)	6.79 (n=1)	
Peritoneum	6.79±0.80 (n=4)	/	/	
Intrapulmonary	1.71±0.74 (n=2)	/	5.68 (n=1)	
Soft tissue	6.55 (n=1)	/	/	

SCC, squamous cell carcinoma; ADC, adenocarcinoma; SCLC, small cell lung carcinoma.

Figures

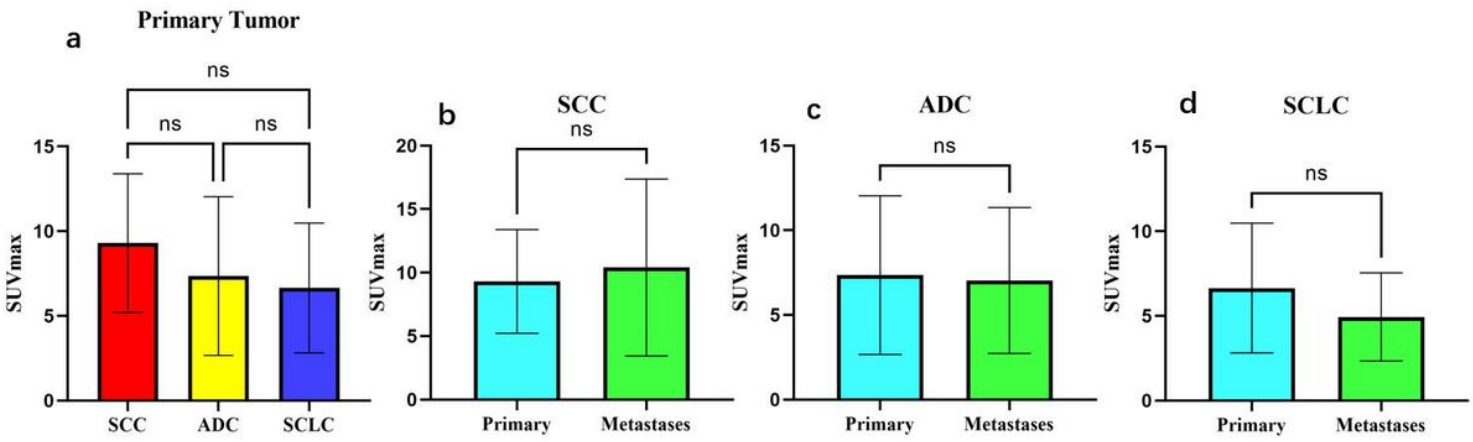

Figure 1

18F-NOTA-FAPI-04 uptake in primary tumors and metastases. ns, not significant.

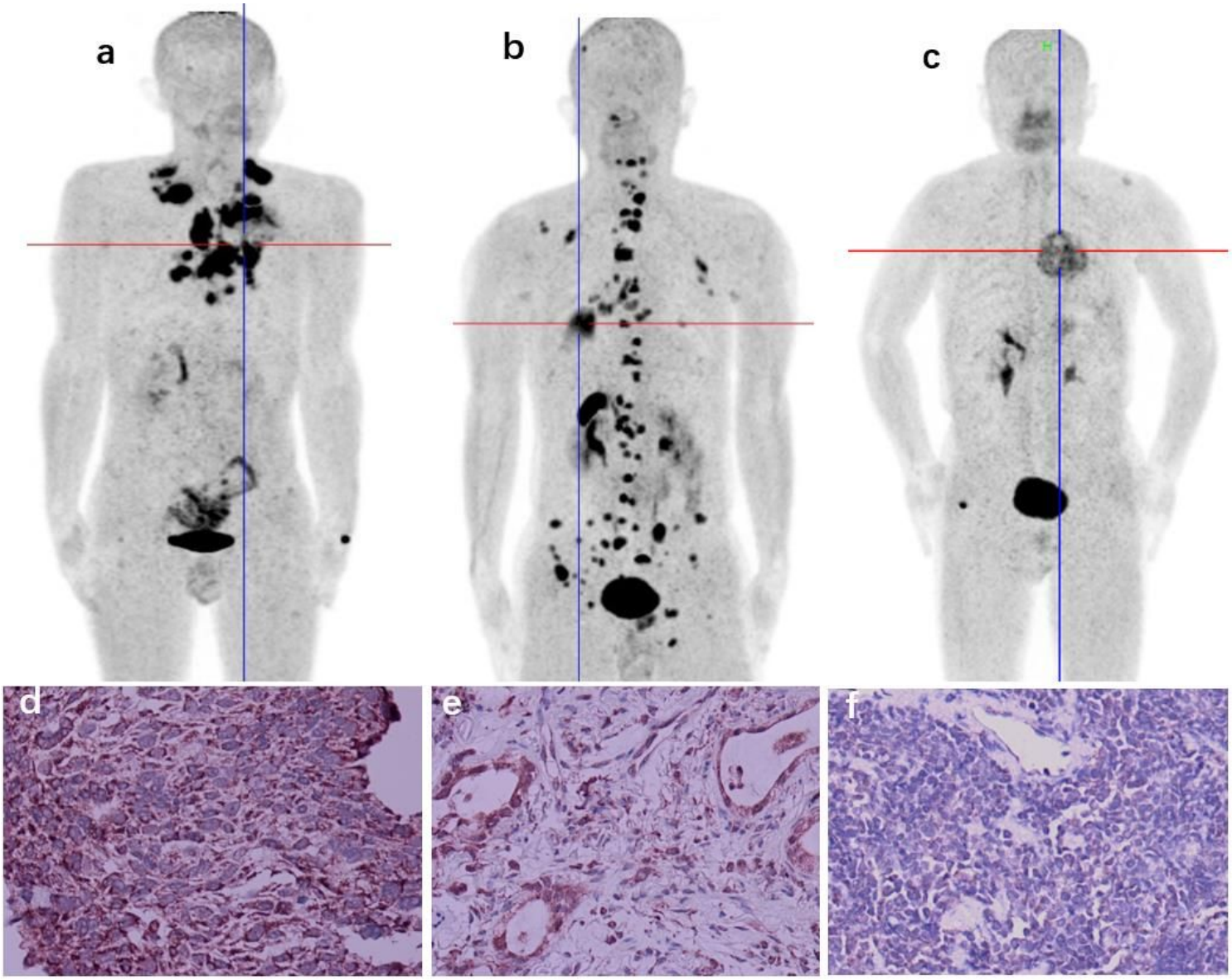

Figure 2

Representative 18F-NOTA-FAPI-04 PET/CT scans from patients with SCC (a: SUVmax=13.64), ADC (b: SUVmax=6.88) and SCLC (c: SUVmax=4.60). d, Strong FAP staining of primary ADC tumor (200×). e, Moderate FAP staining of primary SCC tumor (200×). d, Weak FAP staining of primary SCLC tumor (200×). Primary tumors were located where the red and blue lines cross.

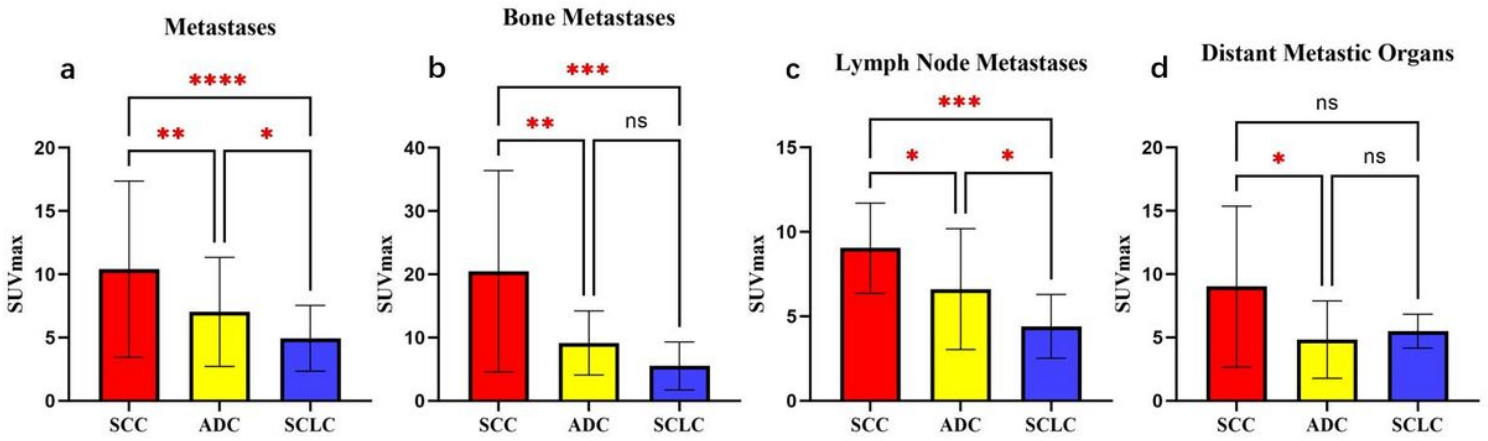

Figure 3

Differences in uptake values between metastases among different pathological types of lung cancer. *, p<0.05; **, p<0.01; ***, p<0.001; ****, p<0.0001.

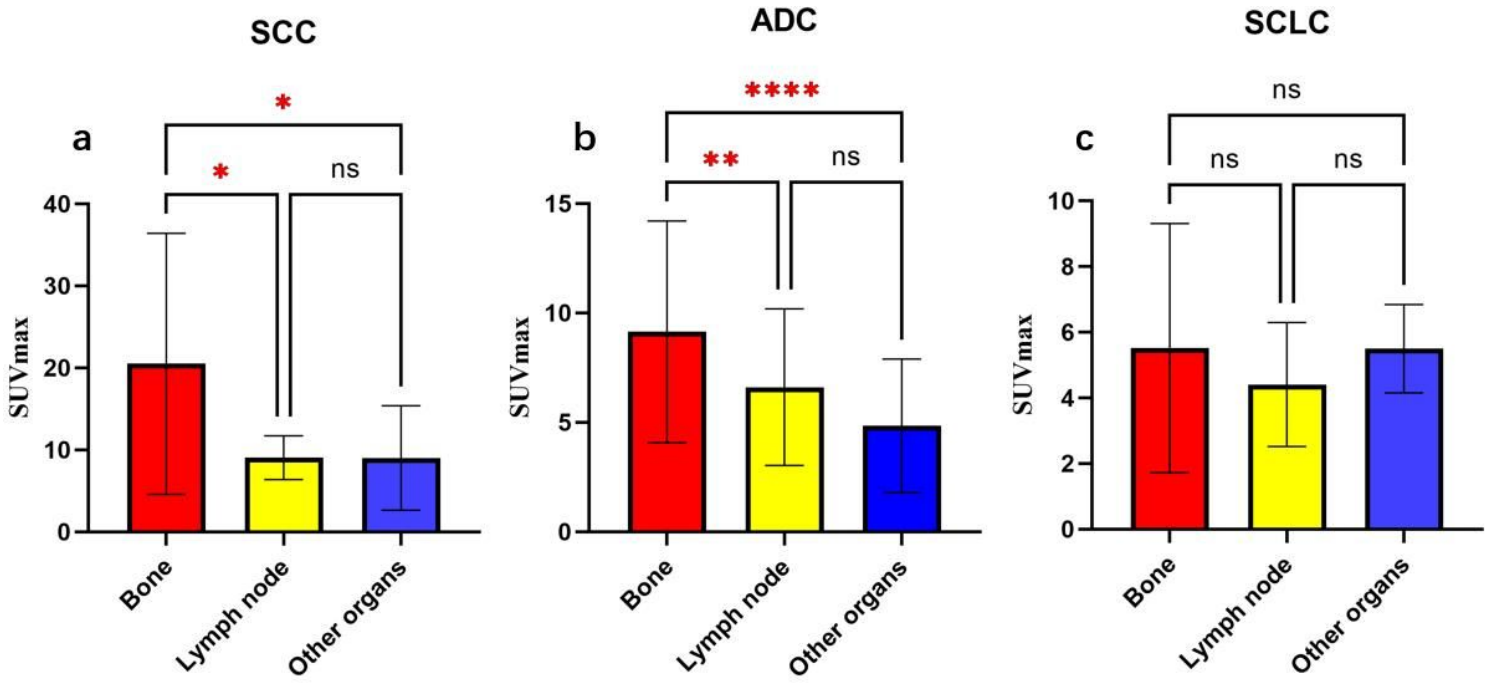

Figure 4

Differences in uptake values between different types of metastases. ns, not significant; *, p<0.05; **, p<0.01; ****, p<0.0001.

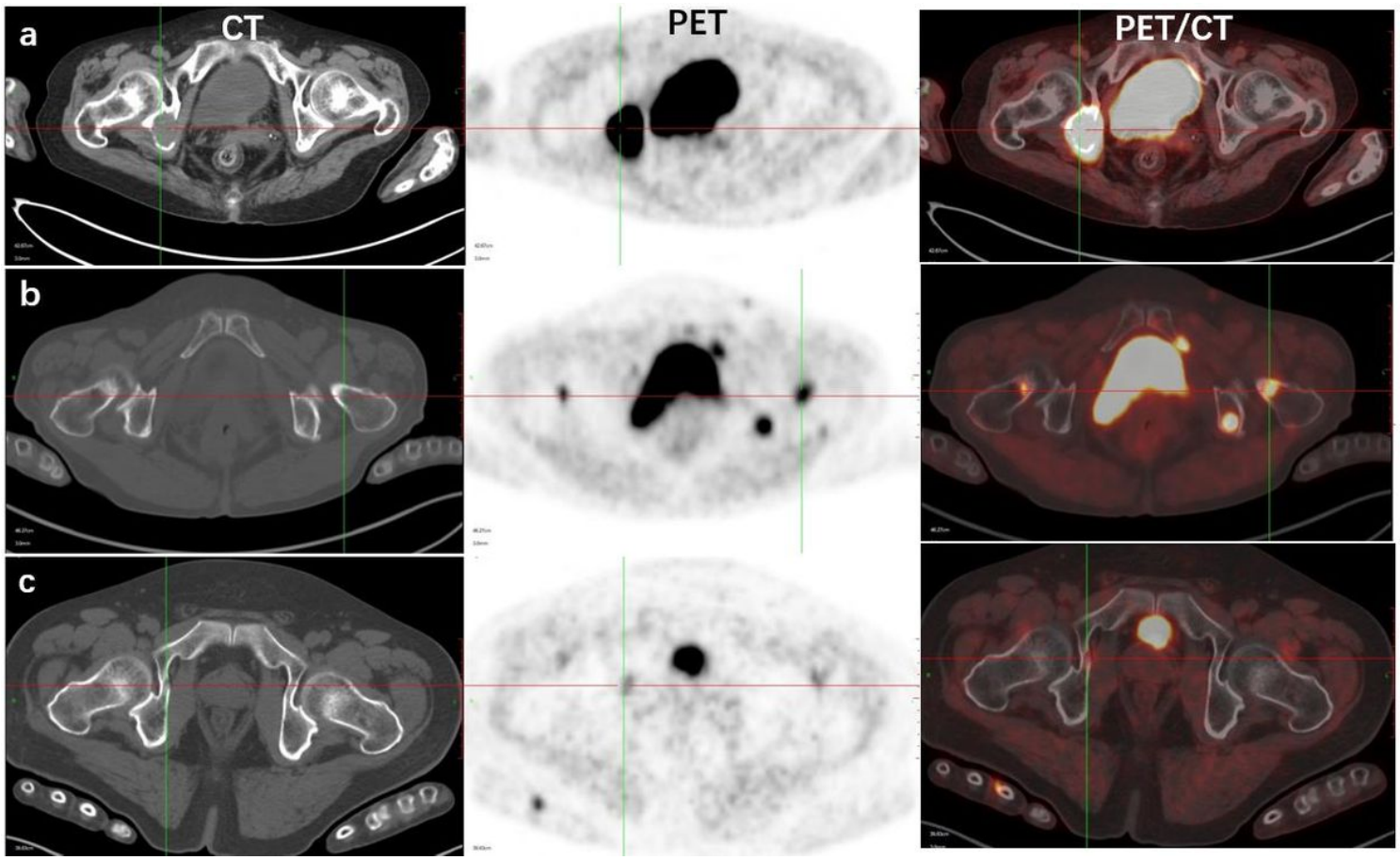

Figure 5

Representative 18F-NOTA-FAPI-04 PET/CT scans of bone metastasis in patients with SCC (a: SUVmax=26.27), ADC (b: SUVmax=13.2) and SCLC (c: SUVmax=6.24). Lines cross at the sites of bone metastasis.